Biogeomorphic influences on river corridor resilience to wildfire disturbances in a mountain stream of the Southern Rockies, USA

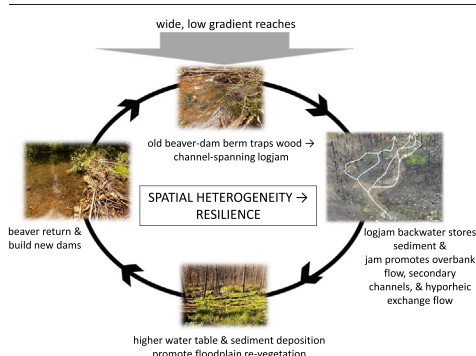Ellen Wohl [a],*, Anna E. Marshall [a], Julianne Scamardo [a], Daniel White [b], Ryan R. Morrison [b]

[a] Department of Geosciences, Colorado State University, Fort Collins, CO 80523-1482, USA
[b] Department of Civil and Environmental Engineering, Colorado State University, Fort Collins, CO 80523-1372, USA

HIGHLIGHTS

- Wildfires create a disturbance cascade from excess water and sediment runoff
- Spatial heterogeneity within a river corridor can attenuate downstream fluxes
- We explore spatial heterogeneity created by logjams and abandoned beaver dams

GRAPHICAL ABSTRACT

ABSTRACT

We examine a 9.4-km-long portion of a montane river corridor in the Southern Rockies, the upper 8 km of which burned in 2020. We focus on sediment storage in logjam backwaters and how spatial heterogeneity in the river corridor attenuates downstream fluxes of material following the wildfire. Wider portions of river corridor exhibit greater spatial heterogeneity, as reflected in multithread channel planform and more closely spaced abandoned beaver dams and channel-spanning logjams. Logjams in multithread reaches have greater volumes of backwater storage and store finer sediment than logjams in single-thread reaches. Despite substantial turnover of sediment in backwater storage during the first runoff season after the wildfire, the cumulative volume of sediment stored at 11 monitored logjams following the 2021 runoff season was 71% of the cumulative sediment volume at the logjams immediately after the fire. Floodplain vegetation regrowth was also faster and more complete at multithread reaches. Vegetation recovery contributed to overbank deposition in these reaches, in contrast to the bank erosion observed in single-thread reaches. More spatially heterogeneous portions of the river corridor appear to be disproportionately important in attenuating enhanced inputs of sediment following wildfire, and the cumulative effect of this attenuation across a river network likely enhances watershed-scale resilience to wildfire disturbance.

1. Introduction

1.1. River corridor geomorphology and the wildfire disturbance cascade

Wildfires create a disturbance cascade in mountainous watersheds. The abrupt alteration of land cover and removal of litter and duff layers of the soil during an intense fire commonly increase water and sediment yields to a river corridor for at least a year following the fire (e.g., Benavides-

* Corresponding author.
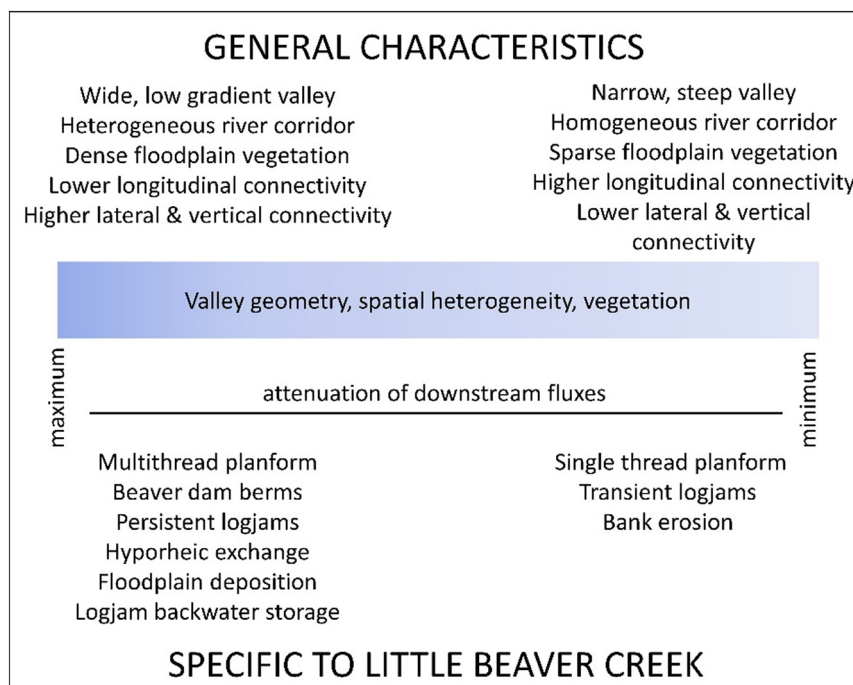E-mail address: ellen.wohl@colostate.edu (E. Wohl).

Solorio and MacDonald, 2001; Moody and Martin, 2001; Murphy et al., 2019; Santi and Rengers, 2020). Increased water and sediment inputs alter flow regime and sediment dynamics in the channel (Rathburn et al., 2018) and can drive changes in channel cross-sectional and planform geometry (Brogan et al., 2019), the abundance and distribution of large wood (Benda et al., 2003; Zelt and Wohl, 2004; Flitcroft et al., 2016), three-dimensional hydrologic connectivity within the river corridor, and two-dimensional (longitudinal, lateral) sediment connectivity (Benda et al., 2003). Higher sediment fluxes from burned watersheds can increase phosphate inputs to water bodies (Coombs and Melack, 2013; Emelko et al., 2016). Along with increased longitudinal connectivity that limits detention and microbial processing of nitrate, this can result in algal blooms in lakes and reservoirs (McEachern et al., 2000; Santin et al., 2018). As a warming climate drives more intense and frequent wildfires in drylands around the world (Westerling et al., 2006), it becomes increasingly important to understand the characteristics that foster resilience to the wildfire disturbance cascade.

We define resilience as the ability to absorb disturbances without diminishing or changing river corridor functions. An example of river corridor functions that could be diminished by a disturbance include decreased hyporheic exchange and associated loss of denitrification as a result of sediment aggradation that buries bedforms such as pools and riffles or removes logjams. We conceptualize resilience as a continuum dependent on specific landforms and processes within the river corridor and the time and space scales of interest. We use river corridor to refer to the active channel(s), floodplain, and underlying hyporheic zone. A river corridor or river network is a system that includes individual components with different levels of resilience. Bedload transport and bed elevation, for example, might vary substantially immediately after a fire but exhibit resilience at timespans of 2–3 years as regrowth of ground cover on adjacent hillsides gradually reduces sediment yield to the river corridor. Channel planform geometry, in contrast, might be resistant to the fire disturbance cascade and show no change, whereas the structure of woody riparian vegetation might require decades to return to pre-fire characteristics.

Both the wildfire disturbance cascade and river corridor resilience to this cascade can be evaluated at the spatial scale of a channel reach or at the scale of an entire watershed. A reach is a length of channel with consistent channel and valley geometry. In smaller channels, reaches might typically be tens of meters long, whereas reaches on large rivers can extend for tens of kilometers. We conceptualize attenuation of downstream fluxes at the scale of individual reaches as fostering watershed-scale resilience. In this context, the cumulative dominance of total channel length by first- to third-order channels (Downing et al., 2012) suggests that reach-scale attenuation by small channels exerts a strong non-linear influence on how the magnitude of the disturbance cascade from adjacent uplands is transmitted downstream, and therefore on watershed-scale resilience to wildfire.

Attenuation within individual reaches varies along a continuum from significantly attenuating downstream fluxes of water and sediment resulting from increased inputs to primarily transmitting these inputs downstream (Fig. 1). Consequently, the manner in which individual reaches respond to the wildfire disturbance cascade governs watershed-scale response. The primary reach-scale influences on attenuation of downstream fluxes are valley geometry, spatial heterogeneity of the river corridor, vegetation, and connectivity (Wohl, 2016; Wohl et al., 2017, 2018). A less laterally confined, lower gradient valley segment has the potential for greater overbank flow, greater channel sinuosity, and the formation of a multithread planform, all of which help to dissipate flow energy and facilitate sediment deposition (e.g., Entwistle et al., 2018). Spatial heterogeneity associated with (i) large wood in the channel and on the floodplain (Sear et al., 2010), (ii) modification of river corridor topography by beavers (*Castor canadensis* in North America, *C. fiber* in Eurasia) (Burchsted et al., 2010), and (iii) diverse floodplain topography created by the history of lateral channel movement can also facilitate dissipation of flow energy and deposition of sediment (e.g., Naiman et al., 2005). Dense riparian vegetation helps to stabilize channel banks and the floodplain surface, as well as dissipating energy and facilitating sediment deposition during overbank flow. Lower longitudinal connectivity and higher lateral and vertical connectivity also help to dissipate flow energy and enhance sediment deposition on the floodplain (Fryirs et al., 2007; Fryirs, 2013; Wohl and Beckman, 2014). Even temporary retention of mineral sediment, pyrogenic carbon, and particulate organic matter attenuates fluxes of phosphorus and nitrogen to downstream water bodies by increasing the potential for microbial uptake of nutrients (e.g., Wollheim et al., 2014).

Fig. 1. A conceptual illustration of our understanding of how geomorphic characteristics of the river corridor attenuate increased inputs of water and sediment following wildfire. The upper level of the diagram describes characteristics of any river corridor and the lower level lists features specifically present in the study area of Little Beaver Creek, Colorado.

The degree to which post-fire inputs of water and sediment overwhelm these characteristics will determine actual, rather than potential, attenuation of downstream fluxes. A low gradient channel with a multithread planform, numerous logjams, dense riparian vegetation, and strong vertical and lateral connectivity, for example, could be changed toward minimum attenuation if a disturbance overwhelms the river corridor. Examples include (i) large peak flows that mobilize the wood and dismantle the logjams (Wohl and Scamardo, 2021); (ii) extensive sediment deposition that blocks off secondary channels and fills pools, creating more efficient sediment transport in the main channel (e.g., Lisle, 1982); or (iii) overbank sediment deposition that is too rapid and thick for floodplain vegetation to regrow quickly or overbank deposition that is sufficiently thick to disconnect the water table from the soil surface (Sparacino et al., 2019). Even a river corridor configuration that maximizes attenuation has some upper disturbance limit on what it can absorb with respect to increased downstream fluxes, so the magnitude and timing of increased water and sediment inputs, and the manner in which characteristics such as spatial heterogeneity, vegetation, and connectivity respond to these inputs, ultimately determine the degree to which an individual reach attenuates wildfire disturbances.

1.2. Logjam attenuation of post-fire sediment flux

Our objective is to use this conceptual framework to examine how the characteristics in Fig. 1 influence reach-scale response of the river corridor to wildfire along a third-order stream draining 40 km² in the Southern Rockies. We examine a 9.4-km-long study reach, of which most of the upper 8 km, along with most of the watershed, burned in 2020. Within this study reach, we focus on the role of channel-spanning logjams in attenuating post-fire sediment fluxes. Previous investigations of changes in riverine large wood dynamics following wildfire have focused on recruitment of fire-killed trees (Jones and Daniels, 2008; Bendix and Cowell, 2010; Praskievicz and Sigdel, 2021); mobility and size distribution of the resulting instream wood (Young, 1994); and how fire-recruited wood can increase instream wood loads (Chen et al., 2005), formation of logjams (Zelt and Wohl, 2004; Vaz et al., 2021), and fish habitat (Burton, 2005). In studies from the western United States, wildfires typically increased wood recruitment and instream wood loads, with associated increases in channel structural complexity (e.g., backwater pool volume and sediment storage). In studies from the Mediterranean region, the details of the size and shape complexity of wood pieces recruited after wildfire strongly influence the effects of the wood on downstream fluxes and channel morphology (Vaz et al., 2013) and the decay status of wood influences microbial and macroinvertebrate colonization (Vaz et al., 2015).

We are aware of only one study that has explicitly evaluated the role of fire-recruited large wood in forming logjams that then attenuate the downstream movement of post-fire sediment inputs to the stream. Investigating post-fire debris flows in a 169-km² watershed in western Montana, USA, Short et al. (2015) documented post-fire sediment deposition in tributary debris flow fans. In the first years after the wildfire, the mainstem river experienced fine-grained aggradation upstream from each fan, incision through the fan, and coarse-grained aggradation downstream. Several years later, nearly the entire channel had aggraded and become finer-grained, including those segments that had started to incise through fans. This change occurred because the instream wood load increased by as much as 50%, facilitating the formation of large logjams that stored sediment and interrupted longitudinal sediment connectivity.
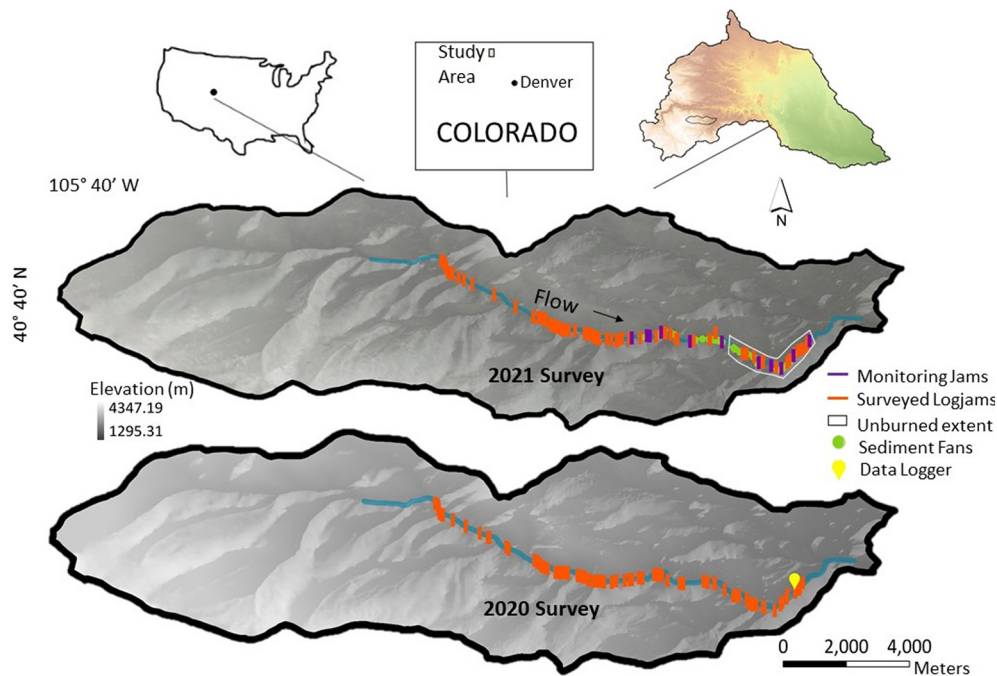
In the watershed that is the focus of our study, there were no post-fire debris flows or massive point sources of sediment into the river corridor. Instead, we observed sediment entering through widespread sheetwash and rill formation on adjacent valley slopes. We use repeat measurements of the volume of sediment stored in multiple logjams to test hypothesized differences in median values for logjam populations in burned versus unburned portions of the river corridor and in more versus less spatially heterogeneous portions of the river corridor. Specifically, we hypothesize that (*H1*) logjams in the unburned zone consistently store more sediment

and finer-grained sediment than logjams in the burned zone or (*H2*) logjams in reaches of greater spatial heterogeneity, regardless of burn status, store more and finer-grained sediment than logjams in reaches of less spatial heterogeneity. This was a late-season wildfire that occurred during base flow and burned logjams in the active channel. Much of the smaller combustible material within the interstices of each logjam was consumed and even large key pieces of wood were partly consumed and weakened. Consequently, the rationale underlying *H1* is that logjams within the burned zone will be less able to withstand the hydraulic force exerted by peak flows and will be more likely to partly or completely breakup than intact logjams in the unburned zone. We assess spatial heterogeneity based on channel planform (single channel vs multithread channel), logjam distribution density (longitudinal spacing of channel-spanning logjams), and presence of abandoned beaver dams as these influence floodplain topography and longitudinal variations in channel width. The rationale underlying *H2* is that dissipation of energy during peak flows as a result of greater hydraulic roughness and division of discharge into multiple smaller channels will result in greater sediment retention in more heterogeneous reaches, regardless of burn status. *H1* tests the idea that burn status is the primary control on logjam backwater storage, whereas *H2* tests the idea that reach-scale geometry is the primary control on this storage. If the analyses support *H2*, this implies that logjams can help to attenuate post-fire sediment fluxes even in burned portions of a watershed.

2. Study area

Little Beaver Creek (LBC) drains 40 km² in the Front Range of Colorado, USA, flowing into the South Fork of the Cache la Poudre River at an elevation of 2400 m (Fig. 2). The watershed is underlain by Precambrian-age Silver Plume Granite (Cole et al., 2010) and has a warm, semiarid climate with mean annual precipitation of 55 cm and mean annual temperature of 8.3 °C (Barry, 1973). Spatially heterogeneous fracture patterns in the granite create downstream alternations at lengths of 10^1–10^2 m between relatively steep, narrowly confined valley segments and lower-gradient, less confined segments. Average channel gradient is 3.6% and floodplain width varies from 15 to 50 m (Table S1). Channel planform alternates downstream between single-thread step-pool channels with boulder substrate in the steep segments to multithread (anastomosing) channels with pool-riffle bedforms or wood-forced steps and pools, and a cobble substrate, in the wider valley segments. Long-term stream gauge records throughout the region indicate that a late spring-early summer snowmelt peak produces the largest runoff volume, but summer convective storms can produce brief floods of higher magnitude (e.g., Jarrett, 1990). The watershed is ungauged but regional regression estimates from the U.S. Geological Survey (streamstats.usgs.gov; Capesius and Stephens, 2009) suggest that the snowmelt peak averages 1.26 m³/s and base flow is 0.15 m³/s. We recorded flow stage at the downstream end of the study area from 8 August 2020 (prior to the wildfire) to 17 October 2021.

Prior to a wildfire in 2020, the LBC watershed included old-growth montane forest dominated by ponderosa pine (*Pinus ponderosa*), with Engelmann spruce (*Picea engelmannii*), Douglas-fir (*Pseudotsuga menziesii*), aspen (*Populus tremuloides*), and willows (*Salix* spp.) also present in the river corridor. Large wood and channel-spanning logjams were abundant along the creek (Jackson and Wohl, 2015) and almost the entire length of the mainstem was affected by beaver modifications. Although only one active beaver lodge and dam were present immediately before the fire, relict beaver dams that are now covered with multi-stemmed willows are abundant along the creek. Although some of these relict dams in the upper part of the watershed still pond substantial amounts of water, most of the relict dams are partly breached. Field surveys indicate that the creek flows through these breaches at a gradient similar to the channel segments immediately up- and downstream, but the remnant flanks of the dam create lateral constrictions that appear to effectively trap large wood moving downstream and facilitate formation of channel-spanning logjams, based on the high proportion of logjams associated with old beaver dams (Table S2). These logjams enhance hyporheic exchange flows (Doughty

Fig. 2. Location map of the study area. Inset at upper right indicates the entire Cache la Poudre River watershed and black outline at lower left within this watershed indicates the Little Beaver Creek watershed. Peak flow was measured at the data logger.

et al., 2020; Ader et al., 2021) and storage of particulate organic matter (Marshall et al., 2020).

The Cameron Peak Fire map indicates that 86% of the watershed burned during the Cameron Peak Fire of August–October 2020, although a small portion (about 1300 m long) of the lower forested portion of the river corridor did not burn (Figs. 2 and S1). A significant portion (68%) of the burned watershed is classified as high or moderate severity, meaning that nearly all the organic ground cover was consumed by the wildfire (Fig. S2). Because this was a late-season fire, LBC was at base flow and even logjams within the active channel burned (Fig. S2). Our study reach extends along the forested portion of the river corridor from the upper beaver meadow to the lower beaver meadow: a cumulative valley length of 8060 m. The logjams indicated in Fig. 2 are bracketed up- and downstream by these beaver meadows.

3. Methods

3.1. Field methods

Following the wildfire, we were first able to access the watershed in November 2020, with only a brief window of time before the creek froze over for winter. We used a handheld Garmin eTrex (±3 m horizontal accuracy) to map the location of all of the channel-spanning logjams between the upper and lower beaver meadows. We categorized each jam with respect to type of key piece. A logjam key piece, analogous to the keystone in an arch, is the largest and most stable piece that tends to trap other, mobile wood pieces to create and maintain a logjam. We assigned logjam key pieces to the categories of ramp (one end resting above bankfull stage), bridge (both ends above bankfull stage), buried (partly within streambed sediment), or pinned (resting at the upstream side of an obstacle such as a large boulder or living tree trunk). We also visually assessed backwater storage of water and fine sediment at each logjam as high (elevated backwater surface across entire channel, minimal velocity in the backwater and substantial trapping of finest sediment and particulate organic matter), medium (elevated backwater surface across at least 70% of channel and associated trapping of fine sediment), or low (backwater effects on flow and sediment across much of the channel, but bed aggradation to the top

of the jam or high jam porosity and permeability limit backwater storage of fine sediment and organic matter).

This initial survey noted 91 channel-spanning logjams, 74 of which were within the burned zone. We then chose 11 jams for more detailed monitoring along 3800 m of the downstream portion of the river corridor. The jams were chosen to reflect the diversity of burned versus unburned riparian corridor; single-thread versus multithread channel planform; and associated, or not, with the berm of an abandoned beaver dam. Six of these jams are in the burned zone and the remainder in the downstream, unburned zone of the river corridor. Starting in April 2021, we measured backwater pool volume, and volume and grain-size distribution of sediment stored in the backwater pool of each monitored jam at approximately bi-weekly intervals until the end of September 2021. We measured backwater volumes and collected samples at each of the 11 monitored logjams 17 times (17 November 2020; 26 April; 7, 14, 20 May; 1, 11, 21, 30 June; 13, 22, 30 July; 5, 11, 24 August; 9, 28 September 2021), for a total of 187 samples of backwater sediment. The measurements of sediment volume included only sediment below the water level and were thus dependent on stage at the time of the field sampling. At the end of the field season, we also measured the total volume of backwater sediment associated with the logjam (Fig. S3). Grain-size distribution was determined from a grab sample taken during each visit. This sample was then oven-dried and sieved and weighed, with particulate organic material and charcoal removed and weighed separately. All sediment in the grab samples was pebble-sized or smaller. We took approximately 200 photographs along the river corridor between the upstream- and downstream-most monitored logjams during each field visit to record changes in channel and valley morphology and regrowth of vegetation on the floodplain. We also resurveyed channel-spanning logjams along the entire length of the creek in October 2021.

In addition to the in-channel measurements, we used the handheld GPS to map the up- and downstream boundaries of multithread versus single-thread channel segments while walking the length of the creek. We chose two valley segments near logjam monitor site 4 to represent these populations. The upstream segment is a steep, single-thread channel and the segment immediately downstream is a lower gradient, multithread channel. In each segment we measured the presence of living vegetation along a grid at 9 dates throughout the summer from first exposure of the ground

after snowmelt (26 April) to the end of the growing season (28 September). The grid consisted of a transect 30 m long. Starting at 0 m, we noted the presence or absence of vegetation at 1 m increments along the transect and at 1 m on either side, for a total sample size of 93 points during each period of measurements (Fig. S4). These observations were designed to note relative rate of regrowth of herbaceous ground cover and deciduous saplings (primarily aspen) on the floodplain in narrow versus wider valley segments.

We used the handheld GPS to map point sources of sediment from the adjacent hillslopes onto the floodplain along one side of the creek. In early October 2021, we estimated the volume of sediment remaining on the floodplain in small fans created by these point sources. We also set up a time-lapse camera (Bushnell Trophy Cam) at logjam monitor point 7, the upstream-most jam in the unburned portion of the study area at the time of the November 2020 survey of all channel-spanning logjams. The camera was motion-triggered and captured high flows, as well as a photo once every hour. The photographs taken by this camera provide insight into the nature of ice breakup in spring, the turbidity levels of flow during snowmelt and the summer convective storms, and the movement of logs within the jam. (As well as the wildlife crossing the path of the camera.)

We recorded flow stage and temperature data at the downstream end of the study area from 8 August 2020 (prior to the wildfire) to 17 October 2021 with an Onset HOBO U20L—01 data logger. The logger was fixed to a rebar stage that was anchored to the streambed. Absolute pressure (kPa) and temperature (°C) were recorded at 30-minute intervals. An ambient logger was also installed, adjacent to the channel, to correct for atmospheric pressure. The resulting gauge pressure was converted to stage (cm) (Fig. 3).

3.2. Analyses

We assessed reach-scale spatial heterogeneity using categorical and continuous variables. Categorical variables were channel planform (single vs multichannel), burn status (burned/unburned), and presence/absence of an abandoned beaver dam at each channel-spanning logjam mapped during the Nov. 2020 and Oct. 2021 longitudinal surveys. The underlying assumption is that both a multichannel planform and the presence of abandoned beaver dams (a high proportion of jams associated with abandoned dams; Table S2) create greater spatial heterogeneity in the river corridor. The continuous variable is longitudinal spacing of logjams, with the assumption that more closely spaced logjams equate to greater spatial heterogeneity.

For the 11 monitored logjams, we used the categorical predictor variables of planform (single or multithread), burn (yes or no), beaver berm (present or absent) and the continuous predictor variables of number of peak flows since previous sample collection and presence of channel-spanning logjam during each sampling date (because many of the logjams broke up, this variable changed at most monitored logjams during the course of the 2021 runoff season). We used the continuous response variables of backwater pool volume, volume of backwater sediment storage, and D_{50} of backwater sediment storage.

A Shapiro-Wilk test of normality showed that logjam distribution density at the reach-scale, and sediment and pool volume and D_{50} at the logjam-scale, were all non-normally distributed. Non-parametric tests were therefore used to analyze the dataset. Most statistical analyses were performed using the R statistical package (R Core Team, 2019). For the longitudinal logjam dataset, logjam distribution density was compared by planform and burn status using a Kruskal-Wallis Rank Sum Test followed by Dunn's (1964) test of multiple comparisons. At the logjam scale, the Wilcoxon Rank Sum statistic was used to distinguish statistical differences in sediment volumes, pool volumes, and D_{50} in burned versus unburned reaches, multi-thread versus single thread reaches, and breached versus not breached logjams. Calculations of the Wilcoxon Rank Sum statistic used all available data from the 11 monitored logjams collected over multiple field visits, because sufficient variability was observed in response variables over time. In the case of these binary comparisons, spatial differences between planforms, burn category, and breach status were of more interest than temporal variations within a logjam. However, to test the influence of flash floods on response variables over the period of study, at-a-site variations were of interest. Therefore, linear mixed-effects models were developed including logjam site ID as a random effect to compare changes in sediment volume at a logjam with the number of flash floods occurring between site visits as well as the cumulative number of flash floods since the beginning of the study period. Mixed-effects models were developed using the lme4 package in R (Bates et al., 2015).
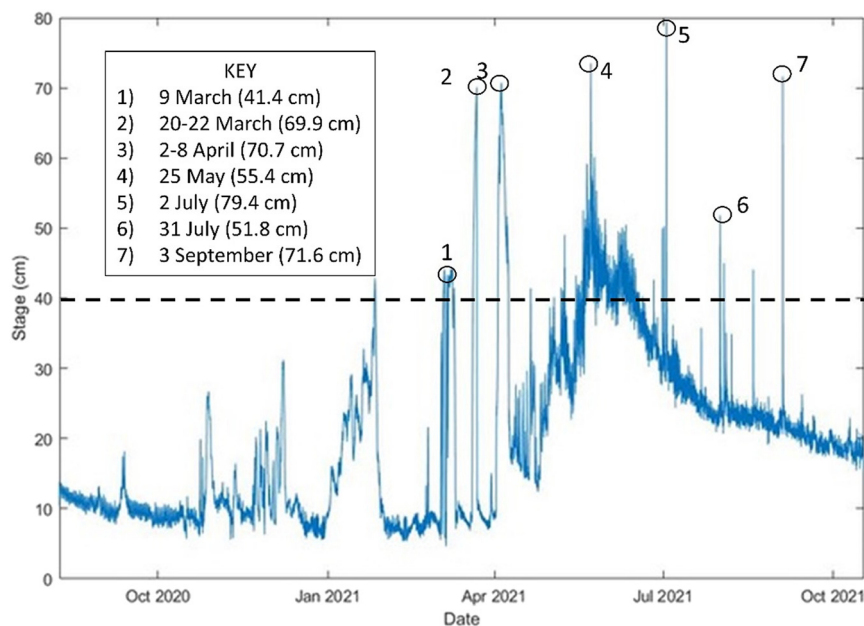

Fig. 3. River stage from 8 August 2020 through 17 October 2021. Threshold of 40 cm used to distinguish peak flows shown by horizontal dashed line. Examples of individual peak flows, with date and peak stage in cm (in parentheses), indicated in inset legend. Water temperatures below freezing were measured periodically from late October 2020 to late April 2021, which may affect stage readings.

4. Results

All of the 187 grab samples of sediment from logjam backwaters included some charcoal and unburned particulate organic matter. The total proportion by weight of these materials varied between samples, from 1% to 40%, but was mostly in the range of 1–10%.

4.1. Flow history during November 2020 to September 2021

Snowmelt runoff peaked on 25 May 2021 at 55.4 cm (1.79 m³/s) on our sensor (Fig. 3). Flash floods associated with convective storms began on 25 June and continued through 3 September 2021. The largest of these peaked at a stage of 79.4 cm (2.7 m³/s) on 2 July. The stage remained above 30 cm in association with snowmelt runoff from 30 April to mid-July. Individual convective storms created elevated stage for between 1 and 5 h. Water temperature dropped below freezing periodically from late October 2020 to late April 2021, indicating the presence of ice in the channel. Pressure measured by the HOBO logger may have been affected by the presence of ice during that time span. However, the elevated stages during March and early April reflect flow over ice, as verified by time-lapse camera photographs. A field visit on 7 April suggested that discharge was not particularly high, but flow on top of an ice layer ~40 cm thick created elevated stage. The ice broke up at about the time of the 7 April field visit, with the exact date varying by location along the channel. Photographs from the time-lapse camera indicate that numerous smaller, short-duration peak flows during July and August were capable of moving bed material and large wood.

The sensor data suggest a shift in base flow magnitude between 2020 and 2021. Although a minor amount of deposition may have occurred in the channel at the sensor location during mid-May, field observations confirm the shift. Six velocity measurements and discharge calculations taken at the sensor site from 13 August 2020 to 17 October 2021 indicate a consistent relation between stage and field-measured discharge, suggesting that base flow has increased during the 2021 runoff season. A similar hydrologic response was observed in a study of 82 watersheds in the western United States (Saxe et al., 2018).

4.2. Sediment inputs to the river corridor

There were no mass movements from the burned slopes within the study area during the 2021 runoff season. During snowmelt, widespread slope wash and minor rills contributed fine sediment throughout the burned length of the river corridor. The series of convective storms that began on 25 June continued to create widespread slope wash but also initiated distinct rills that formed a small alluvial fan where each rill entered the floodplain. These rills and fans became progressively larger with each successive convective storm and, in a few cases, began delivering sand to cobble-sized sediment to the floodplain (Fig. S5). By early October 2021, the 31 fans mapped along one side of the channel within the lower study area around the monitored jams varied in size from <1 to 12 m³ volume and cumulatively stored ~30 m³ of sediment on the floodplain, with an unknown quantity of sediment having entered the active channel(s). We also observed two fans that formed in the unburned area. Sediment in these fans originated in burned areas farther up the valley side slopes, but the sediment in the fans did not reach the active floodplain.

In summary, although snowmelt introduced upland sediment to the river corridor, the formation and progressive increase in small tributary alluvial fans suggest that the magnitude of sediment entering the river corridor increased substantially during the period of convective storms (25 June-3 Sep). The time-interval photographic record strongly suggests that each convective storm created a flash flood with extremely high concentrations of suspended sediment (Fig. S6A). Repeat ground photographs record new marginal channel bars of gravel to cobble-sized sediment (Fig. S6B), indicating that bed-material in at least some portions of the channel was also mobilized during these flash floods.

4.3. Logjam longitudinal distribution through time

There was no precipitation and consequently no wood-mobilizing flows between the time of the 2020 Cameron Peak fire (Aug-Oct 2020) and our initial survey in November 2020. Consequently, we assume that the longitudinal distribution of channel-spanning logjams observed in the first survey reflects the pre-fire distribution of logjams.

Although both the November 2020 and October 2021 logjam surveys tallied a total of 91 logjams, only 38% of the logjams present in 2020 were still present in 2021 (Table S2). In other words, the majority of logjams present during the 2020 survey were dismantled by high flows during the spring and summer of 2021, and the majority of the logjams present during the 2021 survey formed during the preceding spring and summer. Despite the large turnover of logjams, the proportion of logjams present in multithread channel reaches and the proportion of logjams associated with abandoned beaver dams remained consistent (Table S2). A smaller proportion of logjam key pieces were ramps in 2021 and a larger proportion of key pieces were bridges, reflecting post-fire treefall across the active channel. The proportion of logjams in each category of backwater sediment storage changed slightly, toward generally smaller backwater storage in 2021. The bottom row of Table S2 refers to the logjams that persisted from the 2020 to the 2021 survey. Most of these logjams were in unburned portions of the river corridor and the great majority of them were associated with abandoned beaver dams. As for the larger population of logjams during the 2020 and 2021 surveys, the majority of persistent logjams had a moderate level of backwater storage.

For the entire study area, the average logjam distribution density (number of jams/100 m valley length) was 1.1 in both 2020 and 2021. Subdividing the population into categories based on burn status and channel planform reveals more variation (Fig. 4). The highest median logjam distribution density occurs in unburned multithread reaches, followed in descending order by burned multithread, unburned single-thread, and burned single-thread. Unburned multithread sites had statistically higher logjam distribution densities than unburned single-thread ($p = 0.02$) and burned single-thread sites ($p = 0.003$), but not statistically different densities than burned multithread sites, based on the Wilcoxon Rank Sum statistic. Burned multithread sites did not have significantly different logjam distribution densities from unburned or burned single-thread sites ($p > 0.05$ for both). There was no significant change in logjam distribution density by reach type from the 2020 survey to the 2021 survey ($p = 0.47$).

4.4. Single- versus multi-thread channel segments

Multithread segments of the river corridor account for ~12% of total valley-floor length in the study area. These segments tend to have lower
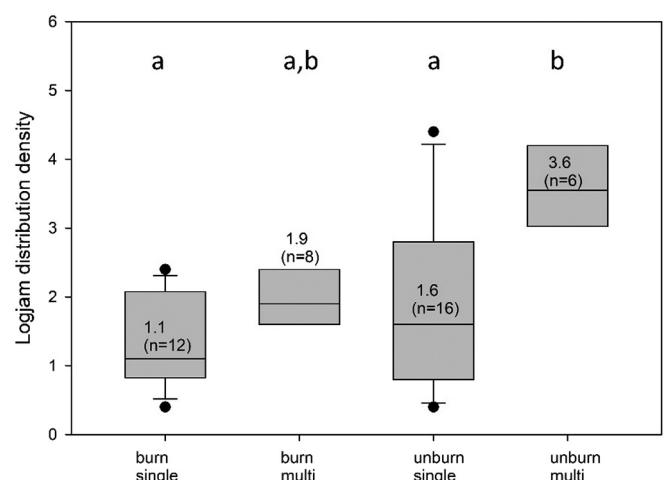

Fig. 4. Logjam distribution density in relation to burn status and channel planform. Median value listed for each population, with sample size in parentheses. Letters a and b indicate statistical similarities and differences among populations.

gradient (average 2%, range 1–3%) than single-thread segments (average 3.6%, range 3–8%). The majority of the abandoned beaver dams also occur in these segments. Prior to the wildfire, we mapped 32 individual beaver dams and 4 reaches (lengths 260, 390, 660, and 860 m, respectively) that contained multiple, closely spaced dams. About half of the individually mapped beaver dams and all 4 of the reaches with large values of logjam distribution density occupy multithread segments.

Our qualitative field observations indicate that most of the observed bank erosion occurred along relatively steep, single-thread portions of the river corridor, whereas overbank deposition was widespread in lower gradient, multi-thread segments (Fig. S7). Most of this erosion and deposition occurred during the summer flash floods, rather than during snowmelt peak flow. Regrowth of herbaceous vegetation and aspen seedlings on the floodplain further enhanced overbank deposition, especially of the finest sediment sizes and coarse particulate organic matter. Regrowth of floodplain vegetation was more rapid and spatially continuous in lower gradient reaches than in steep reaches (Fig. S8).

During the October 2021 re-survey of logjams along the length of the study area, we observed a new, 110-m-long multithread reach forming in association with sediment trapped by large channel-spanning logjams (Fig. S9). We expect this channel planform to persist in subsequent years based on personal field observations elsewhere in the Colorado Front Range.
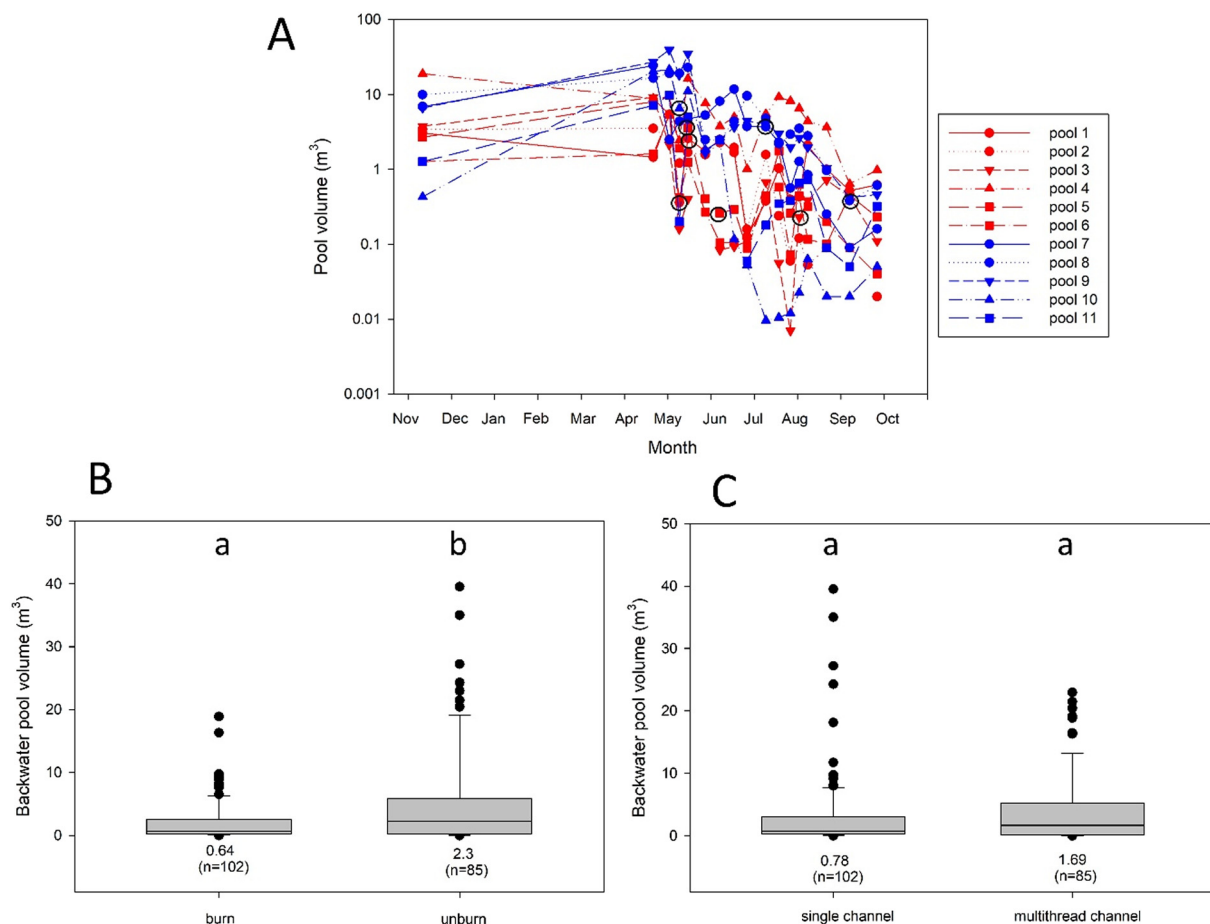
4.5. Logjam and backwater dynamics

The photographs taken during each sampling visit (Fig. S10) can be used to assess logjam dynamics. All of the 11 monitored logjams were quite dynamic. High flows dismantled 9 of the logjams to the point that the logjam no longer spanned the active channel. The date of breach listed in Table S1 represents the first observation during a monitoring visit that the logjam no longer spanned the active channel.

The time-interval camera at logjam monitor point 7 recorded the disappearance of large, key pieces of that logjam and the introduction of new large wood pieces. These exchanges occurred during the snowmelt peak and the subsequent convective storms and flash floods that lasted into early September. New logjams also formed within the study area. We started observing 2 of these new, post-fire logjams in the burned area on 1 June and 22 July 2021, respectively. Each formed where an abandoned beaver dam topped by multi-stemmed willows obstructed downstream transport of large wood pieces (Fig. S11). Although each logjam initially created a large backwater with substantial sediment storage, subsequent flows breached and partly dismantled each logjam and the return of faster velocity in the thalweg upstream from the logjam removed at least some of the backwater sediment. Pebble-sized and finer sediment remained in storage, however, along the margins of the logjam backwater at the end of the 2021 runoff season.

Changes in backwater pool and sediment volumes and backwater sediment grain-size distribution at the 11 monitored logjams can be used to assess backwater dynamics through time. Each of these variables changed between successive sampling visits and did not necessarily exhibit a consistent directional change over the course of the spring and summer. Even with site-specific variations in storage upstream from each logjam, however, backwater pool and sediment volumes significantly decreased as the cumulative number of flash floods increased ($p = 0.0005$ and $p < 0.0001$,

Fig. 5. Backwater pool volumes. (A) Plots of changes in backwater pool volume with time at each of the 11 logjam monitored sites, with sites in burned and unburned portions of the river corridor distinguished as red and blue, respectively. Black circles indicate date of logjam breach. Box plots of backwater pool volumes in (B) burned vs unburned sites and (C) single vs multithread channel planform. Median values listed for each population, with sample size in parentheses. Letters a and b indicate statistical similarities and differences among populations.

respectively). Distinguishing sites as burned versus unburned indicates that the sample population of logjams in the unburned zone had higher median backwater pool volume ($p = 0.01$) and sediment volume ($p = 0.004$, Figs. 5 and 6). Logjams in the burn zone had greater variability in grain size of backwater sediment and coarser backwater sediment ($p < 0.001$, Fig. 7). The D_{50} value of backwater sediment in burned sites varied from sand (0.06–2 mm) to pebble (4–16 mm), whereas the D_{50} of backwater sediment in unburned sites was almost always sand-sized (Fig. 7). Distinguishing sites as single versus multithread channel planform also indicates that logjams in multithread channels have significantly finer backwater sediment ($p = 0.005$), but not statistically greater backwater or pool sediment volumes ($p = 0.44$ and $p = 0.09$, respectively). Distinguishing sites as breached versus unbreached based on the sample date at which the logjam no longer spanned the active channel, the date of breaching does not necessarily correspond to the smallest pool or sediment volume (Figs. 5 and 6) or to the coarsest backwater sediment (Fig. 7). However, comparing sediment volume, pool volume, and D_{50} before breaching or in unbreached logjams to breached logjams shows that breached logjams have significantly smaller sediment volumes ($p < 0.001$), smaller pool volumes ($p < 0.001$), and coarser-grained backwater sediment ($p < 0.001$).
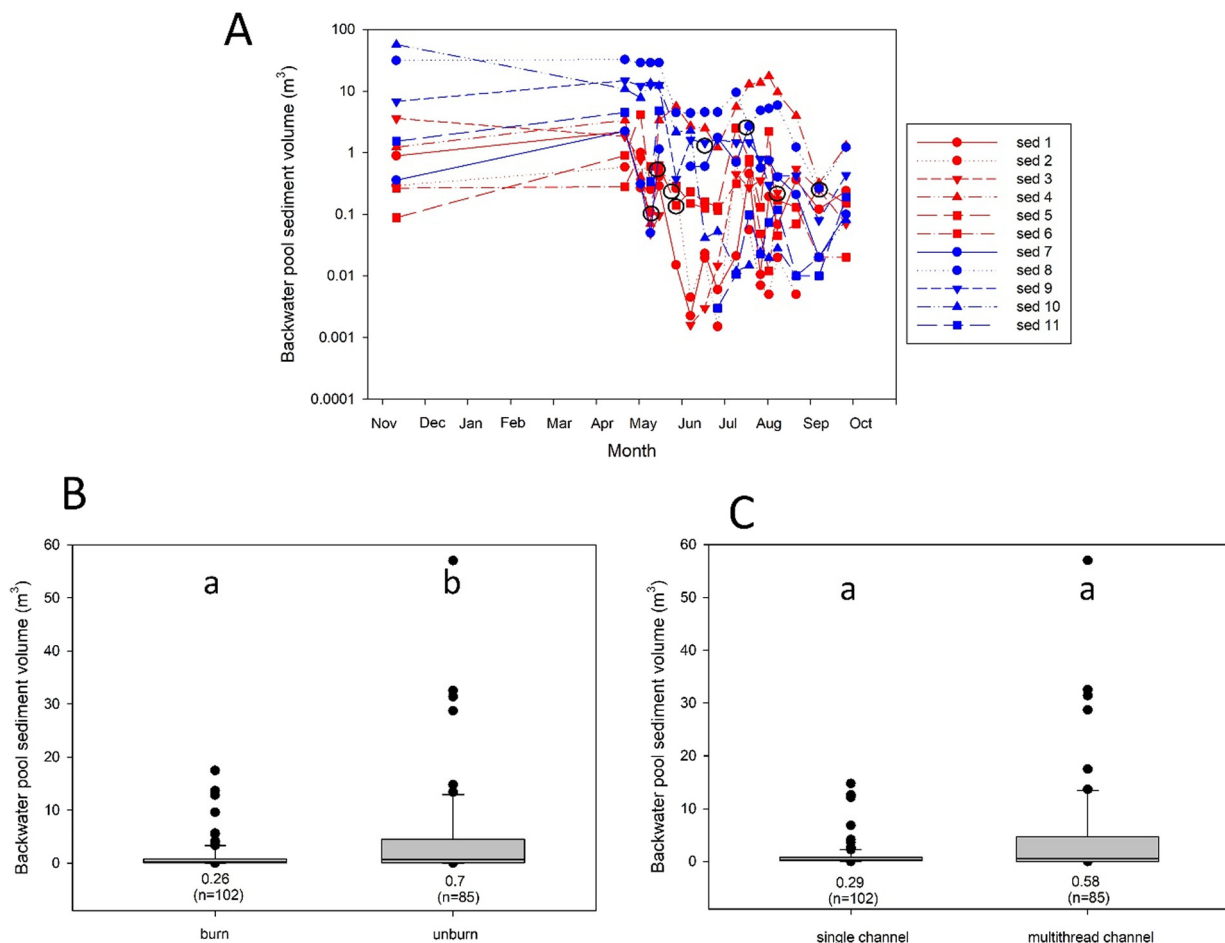
5. Discussion and conclusions

Returning to our original hypotheses, the results suggest that logjams in the unburned zone consistently store more and finer-grained sediment than logjams in the burned zone and that logjams in reaches of greater spatial heterogeneity store finer-grained sediment than logjams in reaches of less spatial heterogeneity. In other words, the results support *H1* relative to *H2* in suggesting that burn status has a stronger influence on individual logjam backwater storage than does reach-scale spatial heterogeneity. However, the greater logjam distribution density in multithread reaches suggests greater reach-scale backwater storage in these reaches than in single-thread reaches, regardless of burn status.
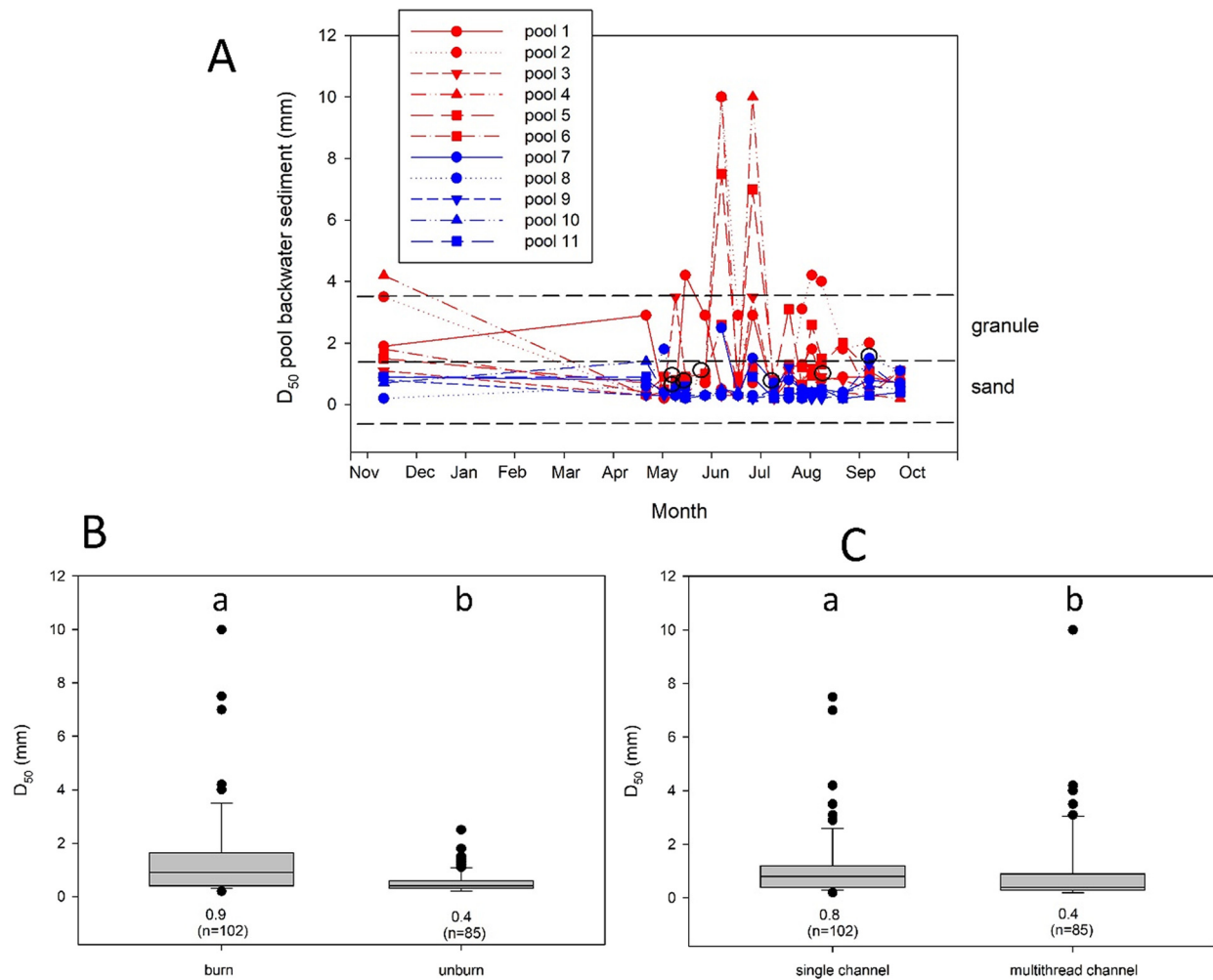
The specific configuration of this creek, with the burned area upstream from the unburned area, may affect the observed patterns in burned versus unburned logjams. We infer that logjams in unburned areas retain more sediment because they have more small material filling the jam interstices and because the unburned logs are less likely to break or to float downstream. If this is correct, unburned logjams should always retain a greater proportion of the sediment reaching them than burned logjams. However, if the unburned logjams were upstream, they would presumably receive far less sediment from adjacent uplands than would logjams in the burned portion of the watershed. Consequently, although the burned logjams might retain a lower proportion of sediment received, they might receive so much more sediment that the net effect would be greater average storage per logjam.

The pattern of sediment movement downstream through time, as reflected in sediment dynamics at the 11 monitored logjams, provides some insight into the magnitude of this sediment storage. Four of the 11 logjams breached as a result of sustained snowmelt peak flow and another 5 breached as a result of summer flash floods. These changes suggest a progressive loss of storage potential in the logjam backwaters. Fluctuations in

Fig. 6. Backwater sediment volumes. (A) Plots of changes in backwater sediment volume with time at each of the 11 logjam monitored sites, with sites in burned and unburned portions of the river corridor distinguished as red and blue, respectively. Black circles indicate date of logjam breach. Box plots of backwater sediment volumes in (B) burned vs unburned sites and (C) single vs multithread channel planform. Median values listed for each population, with sample size in parentheses. Letters a and b indicate statistical similarities and differences among populations.

Fig. 7. Backwater sediment grain size, as represented by D_{50} values. (A) Plots of changes in D_{50} with time at each of the 11 logjam monitored sites, with sites in burned and unburned portions of the river corridor distinguished as red and blue, respectively. Black circles indicate date of logjam breach. Box plots of D_{50} in (B) burned vs unburned sites and (C) single vs multithread channel planform. Median values listed for each population, with sample size in parentheses. Letters a and b indicate statistical similarities and differences among populations.

backwater sediment volumes and the photographic record of each site (Figs. S3 and S10) during the study period indicate substantial turnover of backwater sediment, with sediment present at the time of the wildfire mobilized downstream and new sediment both carried downstream and deposited in each logjam backwater. Despite the instability of the logjams during the first runoff season after the wildfire, the final cumulative sediment volume stored at the logjams at the time of the final survey on 28 September 2021 (74 m^3) was ~71% of the cumulative volume of 103 m^3 stored at the time of the first survey on 7 November 2020 (Fig. S12).

We interpret these results as follows: Sediment volume measured in November 2020 represents pre-fire storage and background levels of sediment yield to the river corridor. Some of the pre-fire sediment stored in the logjams moved downstream during the 2021 runoff season as the logjams became less retentive. However, increased sediment yield to the river corridor after the wildfire suggests that wildfire-related sediment accounted for a greater proportion of the sediment moving downstream during 2021 than pre-fire sediment mobilized from the channel bed. In other words, some pre-fire sediment moved downstream but it was replaced by sediment derived from burned hillslopes. We interpret the volumes of backwater sediment in November 2020 versus September 2021 as indicating that, despite the loss of storage potential at individual logjams, the population as a whole continued to store a substantial amount of sediment and thus effectively attenuated post-wildfire sediment inputs moving down the channel. We assume that if no logjams were present, more of the post-wildfire sediment

inputs would have been transported downstream beyond the study area. This assumption is supported by observations in single-thread reaches without logjams, in which we saw little to no in-channel deposition of pebble-size and finer sediment, reflecting the high transport capacity during snowmelt and convective storm peak flows.

A simple approximation of total sediment storage in logjam backwaters throughout the entire channel length of the study area based on the average backwater storage at the monitored logjams in November 2020 and September 2021 suggests that ~860 m^3 (17 Nov. 2020 value) to 610 m^3 (28 Sep. 2021 value) of sediment were stored in logjam backwaters during the first year following the wildfire. Even if our estimated 30 m^3 of sediment stored in alluvial fans in the river corridor under-represents actual sediment inputs by 1–2 orders of magnitude (which seems reasonable – we did not measure how much sediment entered the active channel), the cumulative logjam backwater storage at the time of the September 2021 survey likely represents a substantial fraction of total sediment inputs to the river corridor.

We did not quantify overbank sediment deposition on the floodplain, but observations of such deposition in wider valley reaches and the presence in these reaches of secondary channels that became inactive after peak flows and thus effectively stored sediment through the summer, together suggest that the combined effects of overbank deposition and deposition in secondary channels likely contribute at least as much sediment storage as main-channel backwaters. Overbank deposits are also more

likely to be persistent than sediment stored in logjam backwaters. We did not observe any subsequent erosion of newly deposited overbank sediment during this first runoff season after the fire, at least in part because fine overbank deposits tended to be rapidly colonized by grasses and herbaceous vegetation that helped to stabilize the sediment (Fig. S7).
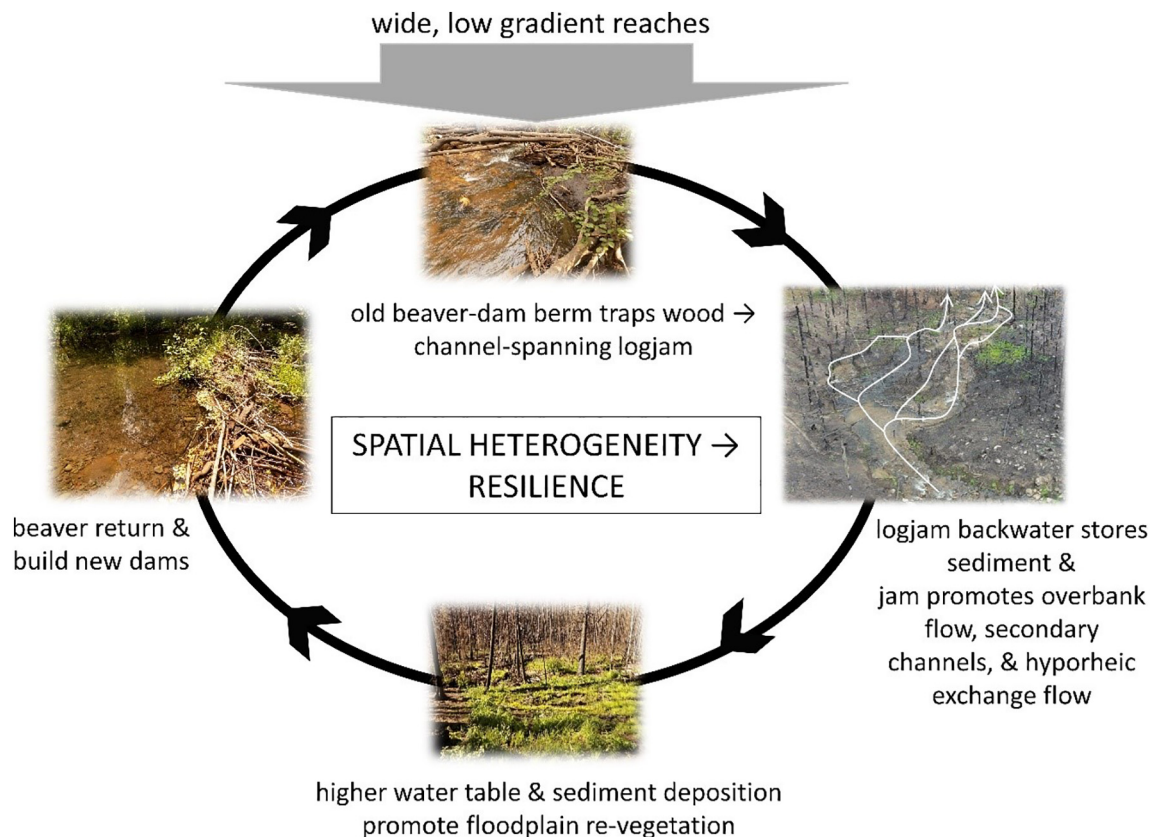
The locations of channel-spanning logjams and old beaver berms correlate with each other, as do the locations of old beaver berms and multithread channel reaches. These correlations are expected: Beaver dams can facilitate formation of a multithread channel planform (John and Klein, 2004; Polvi and Wohl, 2013), as can channel-spanning logjams (Sear et al., 2010; Wohl, 2011). Multithread channel planform equates to smaller channel cross-sectional area within each channel, which can facilitate trapping and retention of large wood pieces (Ruiz-Villanueva et al., 2016) and construction of beaver dams (MacFarlane et al., 2017). These positive feedbacks progressively increase spatial heterogeneity of the river corridor, hydraulic roughness, and thus the potential for attenuating downstream fluxes of water, solutes, and particulate material.

Regrowth of riparian vegetation following the wildfire was more rapid and complete in multithread reaches and we observed predominantly overbank sediment deposition on floodplain surfaces and in secondary channels in multithread reaches. In contrast, we observed predominantly bank erosion in steep, single-thread channel reaches. The 2 monitored logjams that did not breach were in multithread reaches. Logjam distribution density is greater in multithread reaches: ~25% of all of the channel-spanning logjams occurred in the 12% of total valley length formed by multithread reaches (Table S2). Compared to single-thread reaches, logjams in multithread reaches have larger backwaters that store more and finer-grained sediment (although the difference in sediment volume is not statistically significant). All of these observations suggest that the relatively small proportion of total valley length occupied by multithread channel planform creates the greatest reach-scale attenuation of downstream

sediment fluxes and therefore is likely to be disproportionately important in supporting network-scale resilience to the wildfire disturbance cascade.

Although new reaches of multithread channel planform started to form in burned parts of the upper study area, the floodplain geometry did not change substantially during the study period. Multithread channel reaches maintained their capacity to attenuate downstream fluxes, a scenario that was likely helped by the lack of massive point sources of sediment. Despite the large portion of the LBC watershed that burned with a high severity during the Cameron Peak wildfire, summer convective storms in the year following the fire did not trigger large-scale hillslope failures in the form of landslides or debris flows.

This wildfire response that we observed at LBC forms an interesting contrast to another portion of the Poudre River watershed burned during the Cameron Peak fire, the 18.5 km^2 Black Hollow watershed. Black Hollow experienced a massive debris flow on 20 July 2021. The headwaters of Black Hollow are about 6 km (in a straight line that ignores topography) northwest of the LBC headwaters. The enormous, abrupt input of upland sediment caused widespread erosion of the valley floor and impinging terraces and alluvial fans, followed by extensive aggradation of very coarse sediment (including boulders >1 m diameter) during the waning stages of flow. Aerial imagery and ground photographs taken along the valley floor after 20 July by Francis Rengers of the US Geological Survey indicate widespread recruitment of trees to the channel via hillslope and channel-bank erosion. These trees at least temporarily formed logjams that caused upstream sediment aggradation, but most of the logjams subsequently failed, allowing the channel to erode into the aggraded sediment (Fig. S13). Wedges of aggraded sediment extending partway across the valley floor remained present in September 2021, indicating the former location of logjams. Although the logjams failed and released some of the aggraded sediment, the hydraulic roughness and obstructions to flow created by the wood apparently at least partly attenuated downstream sediment

Fig. 8. Conceptual diagram of how interactions in the river corridor create and maintain spatial heterogeneity that fosters reach-scale attenuation of downstream fluxes and network-scale resilience to wildfire disturbance.

fluxes, based on the sediment still present around these features at the end of the 2021 runoff season.

Over the 845 km² burned during the Cameron Peak fire, the Black Hollow watershed has thus far been the only area to experience such a hillslope failure (F. Rengers, US Geological Survey, pers. comm., Jan. 2022). In other words, over much of the burned area, downstream transport of the more diffuse sediment inputs following the wildfire could be strongly affected by the details of valley geometry, spatial heterogeneity, and floodplain vegetation discussed in connection with Fig. 1. And, even after the debris flow in Black Hollow, wider portions of the valley floor that trapped and retained large wood partly attenuated downstream sediment fluxes.

These observations imply that efforts to protect and restore spatially heterogeneous headwater portions of river networks can attenuate downstream fluxes following wildfire and thus enhance resilience to wildfire disturbance at the scale of entire river networks. We have focused on how longitudinal variations in mainstem valley geometry at lengths of 10^1–10^2 m in a 40 km² watershed correspond to greater spatial heterogeneity associated with the history of ecosystem engineering by beavers. Old beaver dams facilitate trapping of large wood and formation of channel-spanning logjams and development of a multithread channel planform (John and Klein, 2004; Polvi and Wohl, 2013). Old dams and logjams facilitate greater lateral connectivity of water, solutes, and particulate material (Sear et al., 2010; Wegener et al., 2017) and greater vertical connectivity of water and solutes (Lautz et al., 2010; Doughty et al., 2020) but reduce longitudinal connectivity (Burchsted et al., 2010). These changes foster a higher riparian water table, dense floodplain vegetation, and overbank sediment deposition (Fig. 8). In other settings, different processes and riverine features could create and maintain spatial heterogeneity of the river corridor. Lateral channel migration that results in partly abandoned channels and floodplain wetlands (Tooth et al., 2002); braided channels in which bars fluctuate in abundance and size in response to changing sediment inputs (Maizels, 1979); tributary alluvial fans that create longitudinal sediment disconnectivity (Fryirs et al., 2007); or logjams that facilitate channel migration and avulsion and create a diverse floodplain mosaic (Collins et al., 2012) are other examples of scenarios that can enhance river corridor heterogeneity and associated attenuation of downstream fluxes.

Floodplains store sediment over diverse timespans and can thus help to attenuate excess sediment inputs following wildfire. The entire river network may not be equally effective, however, in attenuating the greater inputs associated with the wildfire disturbance cascade. Wider reaches with greater spatial heterogeneity, which have elsewhere been described as beads (Stanford et al., 1996; Wohl et al., 2018), are disproportionately important in storing sediment relative to intervening narrow reaches of river corridor. Consequently, river management can potentially reduce the wildfire disturbance cascade and enhance watershed-scale resilience by fostering or maintaining spatial heterogeneity in beads. Spatial heterogeneity reduces longitudinal connectivity and enhances lateral and vertical connectivity, thereby promoting surface and subsurface water storage, as well as storage of sediment and particulate organic matter, and hyporheic exchange flows. Hyporheic exchange, along with even transient sediment and organic matter storage, can reduce inputs of nitrate and phosphate to downstream water bodies after wildfire, thus decreasing another undesirable component of the wildfire disturbance cascade. The smallest streams in a river network both constitute the greatest proportion of channel length and are most closely coupled to adjacent uplands, so the ability of these small streams to attenuate downstream fluxes following wildfire has network-scale consequences for resilience.

Supplementary data to this article can be found online at https://doi.org/10.1016/j.scitotenv.2022.153321.

CRediT authorship contribution statement

Ellen Wohl: Conceptualization, Investigation, Visualization, Writing – original draft, Supervision, Project administration, Funding acquisition. **Anna E. Marshall:** Investigation, Visualization, Writing – review & editing. **Julianne Scamardo:** Investigation, Writing – review & editing. **Daniel White:** Investigation, Visualization, Writing – review & editing. **Ryan R. Morrison:** Investigation, Resources, Supervision, Writing – review & editing.

Declaration of competing interest

The authors declare that they have no known competing financial interests or personal relationships that could have appeared to influence the work reported in this paper.

Acknowledgements

References

Ader, E., Wohl, E., McFadden, S., Singha, K., 2021. Logjams as drivers of transient storage in a mountain stream. Earth Surf. Process. Landf. 46, 701–711.

Barry, R.G., 1973. A climatological transect on the east slope of the front range, Colorado. Arct. Antarct. Alp. Res. 5, 89–110.

Bates, D., Maechler, M., Bolker, B., Walker, S., 2015. Fitting linear mixed-effects models using lme4. J. Stat. Softw. 67, 1–48.

Benavides-Solorio, J., MacDonald, L.H., 2001. Post-fire runoff and erosion from simulated rainfall on small plots, Colorado front range. Hydrol. Process. 15, 2931–2952.

Benda, L., Miller, D., Bigelow, P., Andras, K., 2003. Effects of post-wildfire erosion on channel environments, Boise River, Idaho. For. Ecol. Manag. 178, 105–119.

Bendix, J., Cowell, C.M., 2010. Fire, floods and woody debris: interactions between biotic and geomorphic processes. Geomorphology 116, 297–304.

Brogan, D.J., Nelson, P.A., MacDonald, L.H., 2019. Spatial and temporal patterns of sediment storage and erosion following a wildfire and extreme flood. Earth Surf. Dyn. 7, 563–590.

Burchsted, D., Daniels, M., Thorson, R., Vokoun, J., 2010. The river discontinuum: applying beaver modifications to baseline conditions for restoration of forested headwaters. Bioscience 60, 908–922.

Burton, T.A., 2005. Fish and stream habitat risks from uncharacteristic wildfire: observations from 17 years of fire-related disturbances on the Boise National Forest, Idaho. For. Ecol. Manag. 211, 140–149.

Capesius, J.P., Stephens, V.C., 2009. Regional regression equations for estimation of natural streamflow statistics in Colorado. U.S. Geological Survey Scientific Investigations Report 2009-5136.

Chen, X., Wei, X., Scherer, R., 2005. Influence of wildfire and harvest on biomass, carbon pool, and decomposition of large woody debris in forested streams of southern interior British Columbia. For. Ecol. Manag. 208, 101–114.

Cole, J.C., Trexler, J.H., Cashman, P.H., Miller, I.M., Shroba, R.R., Cosca, M.A., Workman, J.B., 2010. Beyond Colorado's Front Range – a new look at Laramide basin subsidence, sedimentation, and deformation in north-central Colorado. Geological Society of America Field Guide. 18, pp. 55–76.

Collins, B.D., Montgomery, D.R., Fetherston, K.L., Abbe, T.B., 2012. The floodplain large-wood cycle hypothesis: a mechanism for the physical and biotic structuring of temperate forested alluvial valleys in the North Pacific coastal ecoregion. Geomorphology 139–140, 460–470.

Coombs, J.S., Melack, J.M., 2013. Initial impacts of wildfire on hydrology and suspended sediment and nutrient export in California chaparral watersheds. Hydrol. Process. 27, 3842–3851.

Doughty, M., Sawyer, A.H., Wohl, E., Singha, K., 2020. Mapping increases in hyporheic exchange from channel-spanning logjams. J. Hydrol. 587, 124931.

Downing, J.A., Cole, J.C., Duarte, C.M., Middelburg, J.J., Melack, J.M., Prairie, Y.T., et al., 2012. Global abundance and size distribution of streams and rivers. Inland Waters 2, 229–236.

Dunn, O.J., 1964. Multiple comparisons using rank sums. Technometrics 6, 241–252.

Emelko, M.B., Stone, M., Silins, U., Allin, D., Collins, A.L., Williams, C.H.S., Martens, A.M., Bladon, K.D., 2016. Sediment-phosphorus dynamics can shift aquatic ecology and cause downstream legacy effects after wildfire in large river systems. Glob. Chang. Biol. 22, 1168–1184.

Entwistle, N., Heritage, G., Milan, D., 2018. Flood energy dissipation in anabranching channels. River Res. Appl. 34, 709–720.

Flitcroft, R.L., Falke, J.A., Reeves, G.H., Hessburg, P.F., McNyset, K.M., Benda, L.E., 2016. Wildfire may increase habitat quality for spring Chinook salmon in the Wenatchee River subbasin, WA, USA. For. Ecol. Manag. 359, 126–140.

Fryirs, K.A., 2013. (Dis)Connectivity in catchment sediment cascades: a fresh look at the sediment delivery problem. Earth Surf. Process. Landf. 38, 30–46.

Fryirs, K.A., Brierley, G.L., Preston, N.J., Kasai, M., 2007. Buffers, barriers and blankets: the (dis)connectivity of catchment-scale sediment cascades. Catena 70, 49–67.

Jackson, K.J., Wohl, E., 2015. Instream wood loads in montane forest streams of the Colorado front range, USA. Geomorphology 234, 161–170.

Jarrett, R.D., 1990. Paleohydrologic techniques used to define the spatial occurrence of floods. Geomorphology 3, 181–195.

John, S., Klein, A., 2004. Hydrogeomorphic effects of beaver dams on floodplain morphology: avulsion processes and sediment fluxes in upland valley floors (Spessar, Germany). Quaternaire 15, 219–231.

Jones, T.A., Daniels, L.D., 2008. Dynamics of large woody debris in small streams disturbed by the 2001 Dogrib fire in the Alberta foothills. For. Ecol. Manag. 256, 1751–1759.

Lautz, L.K., Kranes, N.T., Siegel, D.I., 2010. Heat tracing of heterogeneous hyporheic exchange adjacent to in-stream geomorphic features. Hydrol. Process 24, 3074–3086.

Lisle, T.E., 1982. Effects of aggradation and degradation on pool-riffle morphology in natural gravel channels, northwestern California. Water Resour. Res. 18, 1643–1651.

MacFarlane, W.W., Wheaton, J.M., Bouwes, N., Jensen, M.L., Gilbert, J.T., Hough-Snee, N., Shivik, J.A., 2017. Modeling the capacity of riverscapes to support beaver dams. Geomorphology 277, 72–99.

Maizels, J.K., 1979. Proglacial aggradation and changes in braided channel patterns during a period of glacier advance: an alpine example. Geogr. Ann. A 61, 87–101.

Marshall, A., Iskin, E., Wohl, E., 2020. Seasonal and diurnal fluctuations of coarse particulate organic matter transport in a snowmelt-dominated stream. River Res. Appl. 37, 815–825.

McEachern, P., Prepas, E.E., Gibson, J.J., Dinsmore, W.P., 2000. Forest fire induced impacts on phosphorus, nitrogen, and chlorophyll a concentration in boreal subarctic lakes of northern Alberta. Canadian Journal of Fisheries and Aquatic Sciences 57, 73–81.

Moody, J.A., Martin, D.A., 2001. Initial hydrologic and geomorphic response following a wildfire in the Colorado front range. Earth Surf. Process. Landf. 26, 1049–1070.

Murphy, B.P., Czuba, J.A., Belmont, P., 2019. Post-wildfire sediment cascades: a modeling framework linking debris flow generation and network-scale sediment routing. Earth Surf. Process. Landf. 44, 2126–2140.

Naiman, R.J., Bechtold, J.S., Drake, D.C., Latterell, J.J., O'Keefe, T.C., Balian, E.V., 2005. Origins, patterns, and importance of heterogeneity in riparian systems. In: Lovett, G.M., Turner, M.G., Jones, C.G., Weathers, K.C. (Eds.), Ecosystem Function in Heterogeneous Landscapes. Springer, NY, pp. 279–309.

Polvi, L.E., Wohl, E., 2013. Biotic drivers of stream planform: implications for understanding the past and restoring the future. Bioscience 63, 439–452.

Praskievicz, S., Sigdel, R., 2021. Loading of stream wood following the 2016 chimney tops 2 wildfire: Great Smoky Mountains National Park, Tennessee, USA. River Res. Appl. 37, 475–483.

R Core Team, 2019. R: A language and environment for statistical computing. R Foundation for Statistical Computing, Vienna, Austria.

Rathbun, S.L., Shahverdian, S.M., Ryan, S.E., 2018. Post-disturbance sediment recovery: implications for watershed resilience. Geomorphology 305, 61–75.

Ruiz-Villanueva, V., Wyzga, B., Hajdukiewicz, H., Stoffel, M., 2016. Exploring large wood retention and deposition in contrasting river morphologies linking numerical modelling and field observations. Earth Surf. Process. Landf. 41, 446–459.

Santi, P.M., Rengers, F.K., 2020. Wildfire and landscape change. Treatise on Geomorphology. 13. Elsevier, pp. 262–287.

Santin, C., Otero, X.L., Doerr, S.H., Chafer, C.J., 2018. Impact of a moderate/high-severity prescribed eucalypt forest fire on soil phosphorus stocks and partitioning. Sci. Total Environ. 621, 1103–1114.

Saxe, S., Hogue, T.S., Hay, L., 2018. Characterization and evaluation of controls on post-fire streamflow response across western US watersheds. Hydrol. Earth Syst. Sci. 22, 1221–1237.

Sear, D.A., Millington, C.E., Kitts, D.R., Jeffries, R., 2010. Logjam controls on channel:floodplain interactions in wooded catchments and their role in the formation of multi-channel patterns. Geomorphology 116, 305–319.

Short, L.E., Gabet, E.J., Hoffman, D.F., 2015. The role of large woody debris in modulating the dispersal of a post-fire sediment pulse. Geomorphology 246, 351–358.

Sparacino, M.S., Rathbun, S.L., Covino, T.P., Singha, K., Ronayne, M.J., 2019. Form-based river restoration decreases wetland hyporheic exchange: lessons learned from the upper Colorado River. Earth Surf. Process. Landf. 44, 191–203.

Stanford, J.A., Ward, J.V., Liss, W.J., Frissell, C.A., Williams, R.N., Lichatowich, J.A., Coutant, C.C., 1996. A general protocol for restoration of regulated rivers. Regul. Riv. 12, 391–413.

Tooth, S., McCarthy, T.S., Brandt, D., Hancox, P.J., Morris, R., 2002. Geological controls on the formation of alluvial meanders and floodplain wetlands: the example of the Klip River, eastern Free State, South Africa. Earth Surf. Process. Landf. 27, 797–815.

Vaz, P.G., Merten, E.C., Warren, D.R., Robinson, C.T., Pinto, P., Rego, F.C., 2013. Which stream wood becomes functional following wildfires? Ecol. Eng. 54, 82–89.

Vaz, P.G., Merten, E.C., Warren, D.R., Durscher, K., Tapp, M., Robinson, C.T., Rego, F.C., Pinto, P., 2015. Fire meets inland water via burned wood: and then what? Freshw. Sci. 34, 1468–1481.

Vaz, P.G., Merten, E.C., Robinson, C.T., Pinto, P., 2021. Severely burned wood from wildfires has low functional potential in streams. J. Appl. Ecol. 58, 1346–1356.

Wegener, P., Covino, T., Wohl, E., 2017. Beaver-mediated lateral hydrologic connectivity, fluvial carbon and nutrient flux, and aquatic ecosystem metabolism. Water Resour. Res. 53, 4606–4623.

Westerling, A.L., Hidalgo, H.G., Cayan, D.R., Swetnam, T.W., 2006. Warming and earlier spring increase western U.S. forest wildfire activity. Science 319, 940–943.

Wohl, E., 2011. Threshold-induced complex behavior of wood in mountain streams. Geology 39, 587–590.

Wohl, E., 2016. Spatial heterogeneity as a component of river geomorphic complexity. Prog. Phys. Geogr. 40, 598–615.

Wohl, E., Beckman, N.D., 2014. Leaky rivers: implications of the loss of longitudinal fluvial disconnectivity in headwater streams. Geomorphology 205, 27–35.

Wohl, E., Scamardo, J.E., 2021. The resilience of logjams to floods. Hydrol. Process. 35, e13970.

Wohl, E., Rathburn, S., Chignell, S., Garrett, K., Laurel, D., Livers, B., Patton, A., Records, R., Richards, M., et al., 2017. Mapping longitudinal stream connectivity in the North St. Vrain Creek watershed of Colorado. Geomorphology 277, 171–181.

Wohl, E., Lininger, K.B., Scott, D.N., 2018. River beads as a conceptual framework for building carbon storage and resilience to extreme climate events into river management. Biogeochemistry 141, 365–383.

Wollheim, W.M., Harms, T.K., Peterson, B.J., Morkeski, K., Hopkinson, C.S., Stewart, R.J., Gooseff, M.N., Briggs, M.A., 2014. Nitrate uptake dynamics of surface transient storage in stream channels and fluvial wetlands. Biogeochemistry 120, 239–257.

Young, M.K., 1994. Movement and characteristics of stream-borne coarse woody debris in adjacent burned and undisturbed watersheds in Wyoming. Can. J. For. Res. 24, 1933–1938.

Zelt, R.B., Wohl, E.E., 2004. Channel and woody debris characteristics in adjacent burned and unburned watersheds a decade after wildfire, Park County, Wyoming. Geomorphology 57, 217–233.